QUANTUM PHYSICS

Cavity-enhanced coherent light scattering from a quantum dot

10.1126/sciadv.1501256

Anthony J. Bennett,[1]* James P. Lee,[1,2] David J. P. Ellis,[1] Thomas Meany,[1] Eoin Murray,[1,3] Frederik F. Floether,[1,3] Jonathan P. Griffths,[3] Ian Farrer,[3†] David A. Ritchie,[3] Andrew J. Shields[1]

The generation of coherent and indistinguishable single photons is a critical step for photonic quantum technologies in information processing and metrology. A promising system is the resonant optical excitation of solid-state emitters embedded in wavelength-scale three-dimensional cavities. However, the challenge here is to reject the unwanted excitation to a level below the quantum signal. We demonstrate this using coherent photon scattering from a quantum dot in a micropillar. The cavity is shown to enhance the fraction of light that is resonantly scattered toward unity, generating antibunched indistinguishable photons that are 16 times narrower than the time-bandwidth limit, even when the transition is near saturation. Finally, deterministic excitation is used to create two-photon N00N states with which we make superresolving phase measurements in a photonic circuit.

INTRODUCTION

Resonant excitation of atoms and ions in macroscopic cavities has led to exceptional control over quanta of light (*1*, *2*), which we aim to translate into the solid state. Engineering cavities around an emitter modifies the local density of optical states, changing the emission pattern and radiative decay rate (*3*). It has been proposed that cavities can also accelerate the rate at which a spin may be prepared (*4*), increase photon-spin coupling (*5*), and enhance Raman scattering (*6*) under resonant optical fields. A reduced radiative lifetime T_1 also leads to an increase in the photon fraction that can be resonantly scattered (*7*, *8*), leading to an "ideal" quantum light source with high efficiency and high coherence.

Three-dimensional pillar microcavities allow a cavity-induced reduction in T_1 by an order of magnitude (*9*–*15*). We resonantly excite and collect photons from the cavity along the axis that couples efficiently to the light field, illustrating the potential of this system as a spin-photon interface and a source of indistinguishable single photons.

RESULTS

Continuous-wave operation

It is possible to suppress the laser signal at the detectors while efficiently collecting the emission from a quantum dot using polarization filtering (Fig. 1A; see the Materials and Methods for further discussion). Until recently, this technique has been limited to optically smooth and flat samples (*16*–*18*), for which a cavity enhancement is not observed. We use a pillar microcavity (Fig. 1B) with a 2.25-μm diameter, which is close to optimal for maximizing the photon extraction efficiency (*10*, *19*). The HE_{11} mode of the device we study has a quality factor, Q, of 8900, which is reduced from the Q of the unetched cavity. Imperfections in the cavity sidewalls that are visible, shown in Fig. 1B, are a possible source of optical loss in the mode (*9*, *19*). By rotating polarizer 2 in the photon detection path, it was possible to suppress the laser collected by a factor of 10^3.

Figure 1D shows data from this microcavity, which contains an X^+ transition emitting photons at 934 nm. Under only resonant illumination (the laser denoted E_r in Fig. 1C) is there an absence of emission from X^+ (red data points, Fig. 1D). However, the addition of <100 pW of illumination at 850 nm (laser E_n) activates the resonant excitation (RE). We attribute this to a single hole captured in the ground state by the process shown in Fig. 1C. This is to be contrasted with the optical gating of neutral excitons, in which it has been reported that resonant excitation (RE) can be suppressed when a charge tunnels into the dot from a nearby defect (*20*). For the device discussed here, the RE collected is increased 500 times by the addition of E_n (Fig. 1D), but the RE can be increased 3000 times in other cavities.

The resonant laser power required to observe RE in these high-Q cavities is about three orders of magnitude lower than that for planar cavities with $Q = 70$ (*21*). This is to be expected given the efficient photon-in-coupling and higher Q. In addition, the Purcell effect has reduced the lifetime of the single-quantum emitter, broadening the transition to $\Delta E = 6.14 \pm 0.19$ μeV (about five times greater than non–cavity-enhanced emitters in this sample).

Figure 2A shows the result of a Hanbury-Brown and Twiss autocorrelation measurement of $g^{(2)}(t)$ recorded under continuous-wave excitation at a Rabi frequency (Ω) of 0.83 GHz. The data are fitted with the well-known equations for $g^{(2)}(t)$ under coherent excitation (*20*, *22*, *23*), including an additional charging-induced bunching effect (*24*). This confirms the dominance of the antibunched quantum emission at the detectors. The spectrum of the RE in Fig. 2B (black data points) appears close to the instrument resolution (0.78 μeV, red line). There is no evidence of the emitter linewidth in this spectrum. This is a clear signature of Resonant Rayleigh Scattering (RRS) by the transition. A least-squares fit gives a spectral width of 0.37 ± 0.03 μeV over the system response; hence, the coherently scattered photons are narrower than the radiative linewidth by a factor of 16.

Figure 2C shows the total intensity, I_{total}, emitted by the transition as a function of Rabi frequency, Ω. One advantage of cavity

[1]Toshiba Research Europe Limited, Cambridge Research Laboratory, 208 Science Park, Milton Road, Cambridge CB4 0GZ, UK. [2]Department of Engineering, University of Cambridge, 9 J. J. Thomson Avenue, Cambridge CB3 0FA, UK. [3]Cavendish Laboratory, University of Cambridge, 19 J. J. Thomson Avenue, Cambridge CB3 0HE, UK.
*Corresponding author. E-mail: anthony.bennett@crl.toshiba.co.uk
†Present address: Department of Electronic and Electrical Engineering, University of Sheffield, Mappin Street, Sheffield S1 3JD, UK.

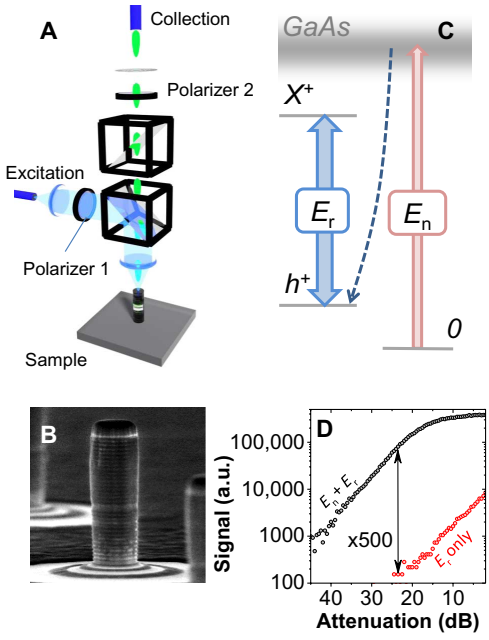

Fig. 1. Resonant excitation of a quantum dot in a microcavity. (**A**) Experimental arrangement. (**B**) Scanning electron microscopy image of a pillar microcavity. (**C**) Energy level diagram with the resonant driving field E_r coupled to the X^+ transition. Resonant emission (RE) can be gated with the weak nonresonant laser, E_n, which creates electron-hole pairs in the GaAs bandgap. Following hole capture in the dot (dashed arrow), the X^+ transition may be resonantly driven. (**D**) Power dependence of the source intensity as a function of the coherent laser intensity, with and without additional excitation by the weak nonresonant laser, E_n.

enhancement is that emission due to RRS, I_{RRS} is greatly increased. The fraction of the total emitted light due to RRS (*7*, *22*) is

$$\frac{I_{RRS}}{I_{total}} = \frac{T_2}{2T_1(1+\Omega^2 T_1 T_2)} \quad (1)$$

where T_1 is the radiative lifetime and $T_2 = 2\hbar/\Delta E$. For an emitter with no cavity enhancement, we typically see $T_1 = 1$ ns and $T_2 = 0.6$ ns (*21*), which would lead to a variation in I_{RRS}, as shown in Fig. 2C (in blue). The maximum fraction I_{RRS}/I_{total} is 0.3, which can only be achieved well below saturation. For a cavity-enhanced source, the fraction I_{RRS}/I_{total} is close to unity (Fig. 2C, red). We observe in Fig. 2B that at $\Omega = 0.83$ GHz, when I_{total} is 0.65 of its maximum value, the RRS dominates the spectrum.

Further confirmation of the character of the emitted light's character can be obtained by two-photon interference measurements. Figure 2D shows the result of a continuous-wave two-photon interference measurement (*12*, *25*) at $\Omega = 0.83$ GHz. Light from the source was passed to a fiber-optic Mach-Zehnder interferometer with a delay of 10.4 ns and a half-wave plate (HWP) in one arm (inset to Fig. 2D). This enabled photons emitted at a time separation of 10.4 ns to take the two paths through the interferometer and meet at the final coupler, C_B. Dependent on the HWP, photons meeting at this coupler can have parallel or orthogonal polarization, and an autocorrelation on the outputs of the interferometer measures the degree of indistinguishability. The difference in the two measurements is quantified by the interference visibility $V_{HOM}(\tau) = (g_{\perp}^{(2)}(\tau) - g_{||}^{(2)}(\tau))/g_{\perp}^{(2)}(\tau)$, which is shown in Fig. 2E. This postselective measurement of two-photon interference is only possible when the detector response time (96 ps) is faster than the coherence time of the photons (*25*), as is the case here. The maximum visibility observed is 0.89, and the

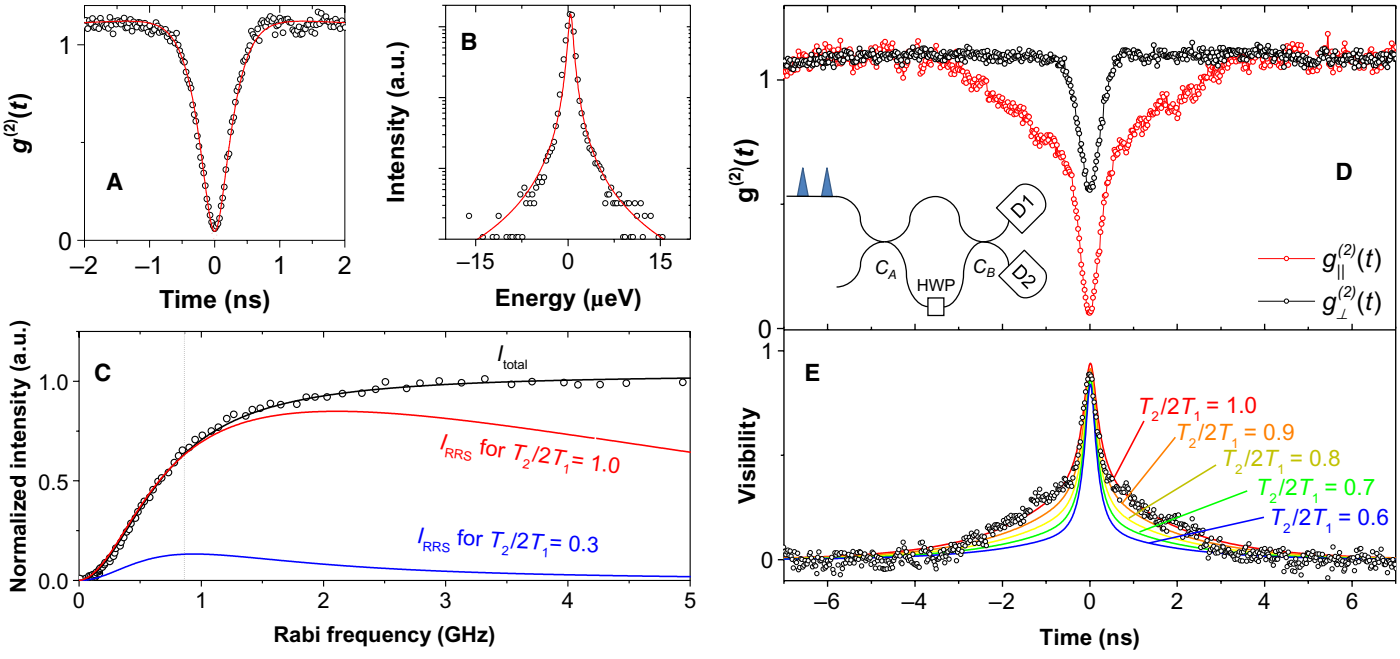

Fig. 2. Cavity-enhanced resonant Rayleigh scattering (RRS). (**A**) Autocorrelation measurement at a Rabi frequency of 0.83 GHz and (**B**) spectrum of the emitted light at the same power (black data points) with instrument resolution (red). (**C**) The power dependence of the emission (black) shown as a function of Rabi frequency. From this, the proportion of the light due to RRS is calculated for $T_2/2T_1 = 1.0$ and 0.3. (**D**) Postselected Hong-Ou-Mandel autocorrelation for parallel (red) and orthogonal (black) photon polarizations. (**E**) Interference visibility deduced from (D), fitted with different values of $T_2/2T_1$.

shape of the visibility plot is determined by the first-order coherence of the photons (*22*). We fit these data (*22*, *26*) for a range of values of $T_2/2T_1$. The calculation provides a remarkably good fit to the data for $T_2/2T_1 = 1.0$. This shows that the source is delivering highly indistinguishable photons and that the Purcell effect has enhanced the RRS part of the spectrum.

Pulsed operation

Next, we discuss the operation of the source under pulsed optical excitation to create on-demand single photons, indistinguishable photon pairs, and N00N states (Fig. 3). Optical pulses of 57 ps length resonantly excite the transition, and Rabi oscillations in the detected RE are observed as a function of the incident field amplitude. The source was driven with 0.71π pulses to provide a near-deterministic excitation and an optimal signal-to-background level (*18*, *21*). When two pulses are used to excite the source at a time separation of 2.36 ns, the emitted photons can again be interfered to determine their indistinguishability. For a pulsed demonstration of two-photon interference, a useful parameter is *g* (*13*), which is the probability of generating two photons in either of the two pulses, divided by the probability of generating two single photons. A measurement of $g = 0.167 \pm 0.005$ is shown in Fig. 3B. For reference, $g^{(2)}(t) = 0.165 \pm 0.004$, where the probability of multiphoton emission during a single laser pulse results in a deviation from the ideal value. When these two photons interfere with parallel or orthogonal polarization (black and red lines, respectively, in Fig. 3C), the difference in coincidences is indicative of a high degree of indistinguishability. Following analysis (*13*), we determine a two-photon overlap, $|\langle\psi_1|\ \psi_2\rangle|^2 = 0.90$.

Finally, we use this source to build a two-photon N00N state, which is the prototypical quantum state used for phase-enhanced measurement (*27*–*29*). The two photons are fed into a silicon oxynitride photonic chip as shown in Fig. 3A, which delivers subwavelength control of path lengths and stability. Two indistinguishable photons interfere at the first coupler and exit together in the superposition state $|2\rangle_A|0\rangle_B + |0\rangle_A|2\rangle_B$. These two paths then experience a relative phase shift, ϕ, transforming the state to $|2\rangle_A|0\rangle_B + e^{2i\phi}|0\rangle_A|2\rangle_B$. Thus, superresolution is achieved because the phase shift introduced to the two-photon state is twice that of a single photon and can be measured by recombining both paths on a final coupler.

Figure 3D shows the single-photon count rate at each output of the photonic chip as a function of the phase shift ϕ when light is only inserted to one of the inputs. The oscillations have a visibility of 0.98, reflecting the balanced splitting of the couplers and the two paths through the interferometer. When two single photons are fed into both inputs, a measurement that postselects two-photon coincidences between the outputs (Fig. 3E) clearly displays a doubled rate of oscillation with phase, relative to the single-photon case. This is the signature of superresolution. The minimum coincidence rate observed in Fig. 3E is determined by the value *g*. Losses in the optics and detectors preclude the observation of phase supersensitivity; thus, this effect is limited to the postselected measurements. However, we anticipate that the future integration of single-photon sources directly onto the chip (*30*) could increase the efficiency of the photon coupling.

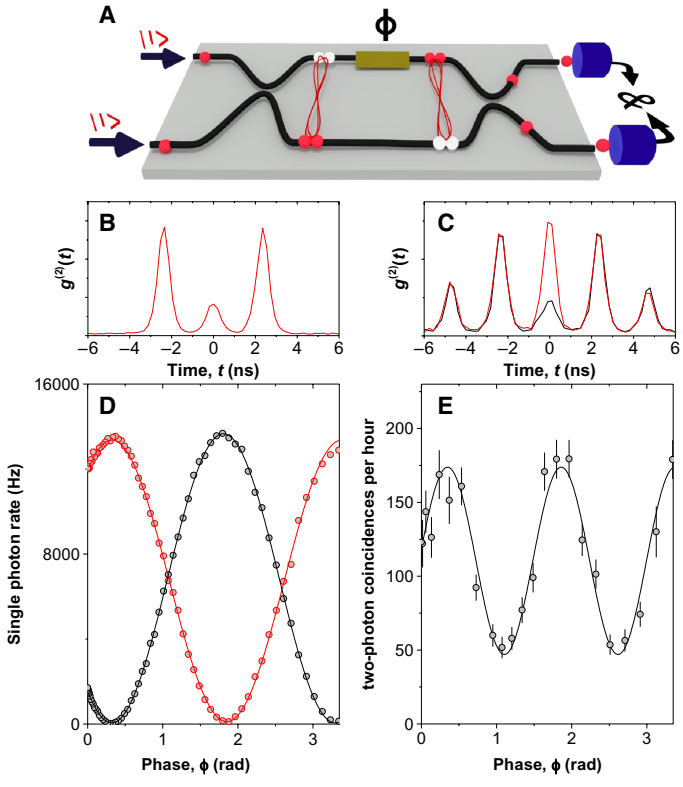

Fig. 3. Deterministic excitation to create on-demand indistinguishable photons and N00N states. (**A**) Schematic of the photonic chip used to generate a two-photon N00N state from two single photons. (**B**) Autocorrelation measurement under pulsed excitation with two laser pulses separated by 2.36 ns. (**C**) Two-photon interference between consecutive single photons with parallel (black) and orthogonal (red) polarization. (**D**) The variation in the single-photon detection rate at the output of the photonic chip as a function of phase, ϕ. (**E**) The two-photon coincidence detection rate at the output of the photonic chip as a function of phase, ϕ.

DISCUSSION

In conclusion, we have demonstrated the coherent excitation of a cavity QED (quantum electrodynamics)–enhanced emitter using the optimal axis for coupling light in and out. We observe indistinguishable coherent photon scattering even as the transition is driven near saturation. Under pulsed, resonant excitation, the high degree of photon indistinguishability can be used to demonstrate superresolution using a N00N state in a photonic chip. These results show how the combination of coherent excitation and cavity QED can lead to a bright and coherent photon source.

MATERIALS AND METHODS

Sample design and measurement optics

The microcavity sample consisted of a Bragg Reflectors with 17 and 26 pairs around a single-wavelength spacer with dots at its center (*14*). The as-grown cavity was designed for 942 nm and was then etched by RIE-ICP (reactive ion etch–inductively coupled plasma) into cylindrical pillars, as shown in Fig. 1B. This sample was mounted inside a closed-cycle cryostat and optically accessed by a custom-built microscope head. Coherent excitation was provided by an attenuated tuneable diode laser. This was directed through linear polarizer 1 and reflected by a pellicle

beam splitter onto the pillar along its symmetry axis. Light was collected along the same direction, transmitted through two pellicle beam splitters before being filtered by polarizer 2, and collected into a polarization-maintaining fiber. In the absence of pellicle or sample birefringence, these polarizers should be set orthogonal to one another to prevent laser light from reaching the detector. However, a transition that couples to the optical field in some incompatible basis (for instance, trion transitions that are circularly polarized) may interact with the input laser and result in finite fluorescence at the detector.

Two-photon interference measurements with pulsed excitation

The data in Fig. 3 were recorded with silicon avalanche photodiodes with a combined timing resolution of 500 ps. Peaks in Fig. 3C were fitted with a double-exponential decay convolved with a Gaussian detector response function. The wave-packet overlap, which is a measure of the visibility that could be achieved when $g = 0$, was determined from the areas of these peaks (*13*). We also performed pulsed two-photon interference measurements with quantum dots in a planar microcavity without Purcell enhancement. In this case, the radiative lifetimes of the charged state were always ~1 ns, but at 5.0 K, it was not possible to observe two-photon interference visibilities under pulsed excitation that were above 0.5 without temporal postselection. In comparison, He *et al.* (*18*) have shown that preselection of a dot with a radiative lifetime of 416 ps (in the absence of Purcell enhancement) can lead to corrected indistinguishabilities, analogous to the photon overlap, of 0.97 ± 0.02.

REFERENCES AND NOTES

1. S. Haroche, J.-M. Raimond. *Exploring the Quantum: Atoms, Cavities and Photons (Oxford Graduate Texts)* (Oxford University Press, Oxford, 2006).
2. D. J. Wineland, Superposition, entanglement, and raising Schrödinger's cat. *Rev. Mod. Phys.* **52**, 10179–10189 (2013).
3. P. Lodahl, S. Mahmoodian, S. Stobbe, Interfacing single photons and single quantum dots with photonic nanostructures. *Rev. Mod. Phys.* **87**, 347 (2015).
4. V. Loo, L. Lanco, O. Krebs, P. Senellart, P. Voisin, Single-shot initialization of electron spin in a quantum dot using a short optical pulse. *Phys. Rev. B* **83**, 033301 (2011).
5. C. Y. Hu, W. J. Munro, J. G. Rarity, Deterministic photon entangler using a charged quantum dot inside a microcavity. *Phys. Rev. B* **78**, 125318 (2008).
6. T. M. Sweeney, S. G. Carter, A. S. Bracker, M. Kim, C. Soo Kim, L. Yang, P. M. Vora, P. G. Brereton, E. R. Cleveland, D. Gammon, Cavity-stimulated Raman emission from a single quantum dot spin. *Nat. Photonics* **8**, 442–447 (2014).
7. H. S. Nguyen, G. Sallen, C. Voisin, P. Roussignol, C. Diederichs, G. Cassabois, Ultra-coherent single photon source. *Appl. Phys. Lett.* **99**, 261904 (2011).
8. K. Konthasinghe, J. Walker, M. Peiris, C. K. Shih, Y. Yu, M. F. Li, J. F. He, L. J. Wang, H. Q. Ni, Z. C. Niu, A. Muller, Coherent versus incoherent light scattering from a quantum dot. *Phys. Rev. B* **85**, 235315 (2012).
9. J. M. Gérard, B. Sermage, B. Gayral, B. Legrand, E. Costard, V. Thierry-Mieg, Enhanced spontaneous emission by quantum boxes in a monolithic Optical microcavity. *Phys. Rev. Lett.* **81**, 1110 (1998).
10. O. Gazzano, S. Michaelis de Vasconcellos, C. Arnold, A. Nowak, E. Galopin, I. Sagnes, L. Lanco, A. Lemaître, P. Senellart, Bright solid-state sources of indistinguishable photons. *Nat. Commun.* **4**, 1425 (2013).
11. A. Ulhaq, S. Weiler, S. M. Ulrich, R. Roßbach, M. Jetter, P. Michler, Cascaded single-photon emission from the Mollow triplet sidebands of a quantum dot. *Nat. Photonics* **6**, 238–242 (2012).
12. S. Ates, S. M. Ulrich, S. Reitzenstein, A. Löffler, A. Forchel, P. Michler, Post-selected indistinguishable photons from the resonance fluorescence of a single quantum dot in a microcavity. *Phys. Rev. Lett.* **103**, 167402 (2009).
13. C. Santori, D. Fattal, J. Vuckovic, G. S. Solomon, Y. Yamamoto, Indistinguishable photons from a single-photon device. *Nature* **419**, 594–597 (2002).
14. M. A. Pooley, D. J. P. Ellis, R. B. Patel, A. J. Bennett, K. H. A. Chan, I. Farrer, D. A. Ritchie, A. J. Shields, Controlled-NOT gate operating with single photons. *Appl. Phys. Lett.* **100**, 211103 (2012).
15. E. Moreau, I. Robert, J. M. Gérard, I. Abram, L. Manin, V. Thierry-Mieg, Single-mode solid-state single photon source based on isolated quantum dots in pillar microcavities. *Appl. Phys. Lett.* **79**, 2865 (2001).
16. C. Matthiesen, A. N. Vamivakas, M. Atatüre, Subnatural linewidth single photons from a quantum dot. *Phys. Rev. Lett.* **108**, 093602 (2012).
17. A. V. Kuhlmann, J. Houel, A. Ludwig, L. Greuter, D. Reuter, A. D. Wieck, M. Poggio, R. J. Warburton, Charge noise and spin noise in a semiconductor quantum device. *Nat. Phys.* **9**, 570–575 (2013).
18. Y.-M. He, Y. He, Y.-J. Wei, D. Wu, M. Atatüre, C. Schneider, S. Höfling, M. Kamp, C.-Y. Lu, J.-W. Pan, On-demand semiconductor single-photon source with near-unity indistinguishability. *Nat. Nanotechnol.* **8**, 213–217 (2013).
19. M. Pelton, C. Santori, J. Vučković, B. Zhang, G. S. Solomon, J. Plant, Y. Yamamoto, Efficient source of single photons: A single quantum dot in a micropost microcavity. *Phys. Rev. Lett.* **89**, 233602 (2002).
20. H. S. Nguyen, G. Sallen, C. Voisin, P. Roussignol, C. Diederichs, G. Cassabois, Optically gated resonant emission of single quantum dots. *Phys. Rev. Lett.* **108**, 057401 (2012).
21. J. P. Lee, A. J. Bennett, J. Skiba-Szymanska, D. J. P. Ellis, I. Farrer, D. A. Ritchie, A. J. Shields, Ramsey interference in a multilevel quantum system. *Phys. Rev. B* **93**, 085407 (2016).
22. C. Cohen-Tannoudji, J. Dupont-Roc, G. Grynberg. *Atom-Photon Interactions: Basic Processes and Applications* (Wiley-VCH, New York, 1998).
23. E. B. Flagg, A. Muller, J. W. Robertson, S. Founta, D. G. Deppe, M. Xiao, W. Ma, G. J. Salamo, C. K. Shih, Resonantly driven coherent oscillations in a solid-state quantum emitter. *Nat. Phys.* **5**, 203–207 (2009).
24. C. Santori, D. Fattal, J. Vučković, G. S. Solomon, E. Waks, Y. Yamamoto, Submicrosecond correlations in photoluminescence from InAs quantum dots. *Phys. Rev. B* **69**, 205324 (2004).
25. R. B. Patel, A. J. Bennett, K. Cooper, P. Atkinson, C. A. Nicoll, D. A. Ritchie, A. J. Shields, Quantum interference of electrically generated single photons from a quantum dot. *Nanotechnology* **21**, 274011 (2010).
26. R. Proux, M. Maragkou, E. Baudin, C. Voisin, P. Roussignol, C. Diederichs, Measuring the photon coalescence time window in the continuous-wave regime for resonantly driven semiconductor quantum dots. *Phys. Rev. Lett.* **114**, 067401 (2015).
27. J. P. Dowling, Quantum optical metrology—The lowdown on high-N00N states. *Contemp. Phys.* **49**, 125–143 (2008).
28. A. N. Boto, P. Kok, D. S. Abrams, S. L. Braunstein, C. P. Williams, J. P. Dowling, Quantum interferometric optical lithography: Exploiting entanglement to beat the diffraction limit. *Phys. Rev. Lett.* **85**, 2733 (2000).
29. J. C. F. Matthews, A. Politi, A. Stefanov, J. L. O'Brien, Manipulation of multiphoton entanglement in waveguide quantum circuits. *Nat. Photonics* **3**, 346–350 (2009).
30. E. Murray, D. J. P. Ellis, T. Meany, F. F. Floether, J. P. Lee, J. P. Griffiths, G. A. C. Jones, I. Farrer, D. A. Ritchie, A. J. Bennett, A. J. Shields, Quantum photonics hybrid integration platform. *Appl. Phys. Lett.* **107**, 171108 (2015).

Acknowledgments

Funding: The Engineering and Physical Sciences Research Council (EPSRC) partly funded the molecular beam epitaxy machine used to grow the sample. E.M. and T.M. acknowledge support from the EU Marie Curie Initial Training Network PICQUE (Photonic Integrated Compound Quantum Encoding) through grant no. 608062. J.P.L. acknowledges support from the EPSRC Centre for Doctoral Training in Photonic Systems Development. **Author contributions:** The microcavity sample was made by D.J.P.E., I.F., and D.A.R. The silicon oxynitride device was made by D.J.P.E., T.M., E.M., F.F.F., and J.P.G. The experiments were performed by J.P.L. and A.J.B. A.J.B. and A.J.S. conceived the experiment and guided the work. The paper was written by A.J.B. with contributions from all authors. **Competing interests:** The authors declare that they have no competing interests. **Data and materials availability**: All data needed to evaluate the conclusions in the paper are available at https://www.repository.cam.ac.uk/handle/1810/253126.

Submitted 10 September 2015
Accepted 25 March 2016
Published 22 April 2016
10.1126/sciadv.1501256

Citation: A. J. Bennett, J. P. Lee, D. J. P. Ellis, T. Meany, E. Murray, F. F. Floether, J. P. Griffths, I. Farrer, D. A. Ritchie, A. J. Shields, Cavity-enhanced coherent light scattering from a quantum dot. *Sci. Adv.* **2**, e1501256 (2016).

ScienceAdvances
AAAS

Cavity-enhanced coherent light scattering from a quantum dot

Anthony J. Bennett, James P. Lee, David J. P. Ellis, Thomas Meany, Eoin Murray, Frederik F. Floether, Jonathan P. Griffths, Ian Farrer, David A. Ritchie and Andrew J. Shields (April 22, 2016)

Sci Adv 2016, 2:.
doi: 10.1126/sciadv.1501256